Progress In Electromagnetics Research B, Vol. 11, 1–14, 2009

EVALUATION OF A NEURAL-NETWORK-BASED ADAPTIVE BEAMFORMING SCHEME WITH MAGNITUDE-ONLY CONSTRAINTS

G. Castaldi and V. Galdi

Waves Group, Department of Engineering
University of Sannio
Corso Garibaldi 107, I-82100 Benevento, Italy

G. Gerini †

TNO Defense, Security and Safety
P.O. Box 96864, 2509 JG, The Hague, The Netherlands

Abstract—In this paper, we present an adaptive beamforming scheme for smart antenna arrays in the presence of several desired and interfering signals, and additive white Gaussian noise. As compared with standard schemes, the proposed algorithm minimizes the noise and interference contributions, but enforces *magnitude-only* constraints, and exploits the array-factor phases in the desired-signal directions as further optimization parameters. The arising nonlinearly-constrained optimization problem is recast, via the Lagrange method, in the unconstrained optimization of a non-quadratic cost function, for which an iterative technique is proposed. The implementation via artificial neural networks is addressed, and results are compared with those obtained via standard schemes.

1. INTRODUCTION

In modern multi-objective radar and communication systems for civilian and military applications, there is an increasing interest toward *smart antennas* [1, 2], capable of processing multiple signals, adapting to possible scenario variations, and mitigating the effects

† Also with Department of Electrical Engineering, Technical University of Eindhoven, 5612 AZ Eindhoven, The Netherlands.

of the background noise and coherent interfering signals arising from multipath and/or (un)intentional disturbances (see, e.g., [3–8]).

Within this context, typical *beamforming* algorithms [1, 2], are based on maximum-likelihood criteria, on the maximization of the signal-to-noise ratio, and on the minimization of the mean square error (MSE) [9]. In particular, MSE-based approaches are based on the minimization of the noise and interference contributions while maintaining a specific array-factor gain in the desired-signal directions. The applicability of the above algorithms is subject to the knowledge of the amplitudes and directions of the desired and interfering signals impinging on the array, which are likely unknown *a priori* and, however, time-varying. In this framework, standard algorithms for the estimation of the direction of arrival, such as MUSIC [10] and ESPRIT [11], are too computationally-demanding for real-time applications. This has motivated a growing interest toward implementations based on *artificial neural networks* (ANNs) [12], which are capable, via suitable *training* procedures, of accurately approximating complex nonlinear mappings, and admit very-large-scale-integration *hardware* implementations. ANN-based algorithms have been successfully applied to several electromagnetics engineering optimization/synthesis problems (see, e.g., [13–15]) and, in particular, to adaptive beamforming schemes based on linearly-constrained MSE minimization [16, 17].

In this paper, we propose an alternative scheme based on the MSE minimization which, unlike those in [16, 17], involves *magnitude-only* (nonlinear) constraints on the array-factor in the desired-signal directions. As compared with the scheme in [16, 17], for each constraint, we recover a real degree of freedom (array-factor phase) which we exploit in the optimization process for performance improvement. Via the Lagrange theory of constrained optimization [18], we reduce the problem to the unconstrained optimization of a non-quadratic functional (depending on the above auxiliary phase unknowns), for which we propose an iterative solution scheme. Moreover, we address the ANN implementation, and assess the overall performance by comparison with standard schemes [16, 17].

In our prototype investigation, we consider a simplified scenario involving a linear array of N isotropic elements in the presence of $M \lesssim N$ narrow-band plane-wave signals with identical center-frequency, and a wide-sense stationary, zero-mean, white Gaussian background noise. The indexes $m = 1, \ldots, M_D$ tag the M_D *desired* signals, which are assumed to all have unit amplitude and *known* incidence directions $\theta_1, \ldots, \theta_{M_D} \in (-90°, 90°)$ from broadside; the indexes $m = M_D + 1, \ldots, M$ tag the $M_I = M - M_D$ *interfering* signals, which

are assumed to all have amplitude Λ and *unknown* incidence directions $\theta_{M_D+1}, \ldots, \theta_M \in (-90°, 90°)$. Moreover, we assume that the elements are uniformly spaced by half-wavelength (at the center-frequency), and that the desired and interfering signals and the noise are mutually uncorrelated. Hence, the array output can be parameterized in terms of an N-dimensional complex vector $\mathbf{r}$ of components

$$r_n(t) = \sum_{m=1}^{M} s_m(t) \exp\left[-j(n-1)\pi \sin\theta_m\right] + \xi_n(t), \quad n = 1, \ldots, N, \tag{1}$$

where $j = \sqrt{-1}$ denotes the imaginary unit, $s_m(t)$ denotes the m-th signal, and $\xi_n(t)$ is a zero-mean Gaussian process with variance σ^2. Equation (1) can be recast in the following compact matrix form [16, 17],

$$\mathbf{r}(t) = \mathbf{A} \cdot \mathbf{s}(t) + \boldsymbol{\xi}(t), \tag{2}$$

where $\mathbf{s} = [s_1, \ldots, s_M]^T$, $\boldsymbol{\xi} = [\xi_1, \ldots, \xi_N]^T$, with the superscript ^{T} denoting the transpose, and $\mathbf{A} = [\mathbf{a}_1, \ldots, \mathbf{a}_M]$ is the $N \times M$ steering (Vandermonde-type) matrix in the direction of the arriving signals [16, 17], constituted by N-dimensional column vectors

$$\mathbf{a}_m = \left[1, \exp\left(-j\pi \sin\theta_m\right), \ldots, \exp\left[-j(N-1)\pi \sin\theta_m\right]\right]^T, \quad m = 1, \ldots, M. \tag{3}$$

The beamforming output y can accordingly be expressed as a suitable linear transformation of the vector $\mathbf{r}$,

$$y(t) = \mathbf{w}^H \cdot \mathbf{r}(t) = \mathbf{w}^H \cdot \mathbf{A} \cdot \mathbf{s}(t) + \mathbf{w}^H \cdot \boldsymbol{\xi}(t), \tag{4}$$

where $\mathbf{w}$ is the N-dimensional complex weight vector (to be determined according to a suitable optimality criterion), and the superscript ^{H} denotes conjugate transpose.

2. PROPOSED SCHEME

2.1. Beamforming Algorithm

Among the various beamforming schemes (and corresponding optimality criteria) available in the literature [2], here we focus on the class of algorithms based on Capon's method [9], which was generalized

in [16, 17] to the case of multiple desired signals. Such algorithms are based on the minimization of the mean output power,

$$P(\mathbf{w}) = \mathbf{w}^H \cdot \mathbf{R} \cdot \mathbf{w}, \tag{5}$$

with *unit-gain* constraints in the directions of the desired signals,

$$\mathbf{w}^H \cdot \mathbf{a}_m = 1, \quad m = 1, \ldots, M_D. \tag{6}$$

In (5), $\mathbf{R}$ represents the $N \times N$ correlation matrix,

$$\mathbf{R} = E\left[\left\langle \mathbf{r}(t) \cdot \mathbf{r}^H(t) \right\rangle\right] = \mathbf{A} \cdot \mathbf{S} \cdot \mathbf{A}^H + \sigma^2 \mathbf{I}, \tag{7}$$

with $E[\cdot]$ and $\langle \cdot \rangle$ denoting the statistical expectation and time average, respectively, $\mathbf{S}$ denoting the $M \times M$ correlation matrix pertaining to the desired and interfering signals (diagonal, in view of the uncorrelation assumption), and $\mathbf{I}$ denoting the $N \times N$ identity matrix. In view of the *complex* (and, hence, *linear*) nature of the constraints in (6), the optimization problem admits a simple *closed-form* solution (see [16, 17] for details). However, it should be emphasized that each complex constraint reduces of *two units* the total number of real degrees of freedom [real and imaginary parts of the weight coefficients in (4)] to be exploited in the optimization process. With the aim of improving the algorithm performance, our proposed scheme is based on the minimization of the same cost function as in (5), but with the enforcement of the unit-gain condition via *magnitude-only* constraints, viz.,

$$\left|\mathbf{w}^H \cdot \mathbf{a}_m\right| = 1, \quad m = 1, \ldots, M_D. \tag{8}$$

As compared with the standard strategy [16, 17] based on the minimization of (5) subject to (6), for each desired signal, we recover one extra real degree of freedom exploitable in the optimization process. However, the *nonlinear* constraints in (8) render the optimization problem more complicated. In this framework, it is expedient to rearrange (8) as

$$\begin{cases} \mathbf{w}^H \cdot \mathbf{a}_m = \zeta_m \\ |\zeta_m|^2 = 1 \end{cases}, \qquad m = 1, \ldots, M_D, \tag{9}$$

where ζ_m are auxiliary unit-magnitude complex unknowns (and, hence, equivalent to real phase variables). By exploiting the Lagrange theory of constrained optimization [18], the minimization of (5) subject to (9) can be reduced to the unconstrained minimization of the Lagrangian

function

$$\mathcal{L}(\mathbf{w};\boldsymbol{\alpha},\boldsymbol{\beta},\boldsymbol{\zeta}) = \mathbf{w}^H\cdot\mathbf{R}\cdot\mathbf{w} - 2\mathrm{Re}\left\{\left(\mathbf{w}^H\cdot\mathbf{A}_D - \boldsymbol{\zeta}^H\right)\cdot\boldsymbol{\alpha}\right\} - \sum_{m=1}^{M_D}\beta_m\left(|\zeta_m|^2-1\right), \tag{10}$$

where the symbol $\mathrm{Re}\{\cdot\}$ denotes the real part, $\mathbf{A}_D = [\mathbf{a}_1,\ldots,\mathbf{a}_{M_D}]$ denotes the $N\times M_D$ steering matrix pertaining to the desired signals, $\boldsymbol{\alpha} = [\alpha_1,\ldots,\alpha_{M_D}]^T$ and $\boldsymbol{\beta} = [\beta_1,\ldots,\beta_{M_D}]^T$ are Lagrange multipliers, and $\boldsymbol{\zeta} = [\zeta_1,\ldots,\zeta_{M_D}]^T$. Since, for $\sigma > 0$, the correlation matrix $\mathbf{R}$ in (7) is strictly positive-defined (and hence invertible), it is easily verified that the unique stationary point of the Lagrangian in (10) with respect to $\mathbf{w}$ is given by

$$\mathbf{w}^{(s)} = \mathbf{R}^{-1}\cdot\mathbf{A}_D\cdot\boldsymbol{\alpha}. \tag{11}$$

By substituting the stationary solution (11) in the constraints (9), we obtain a linear system of equations relating the α-multipliers to the auxiliary unknowns, viz.,

$$\mathbf{B}\cdot\boldsymbol{\alpha} = \boldsymbol{\zeta}, \tag{12}$$

where

$$\mathbf{B} = (\mathbf{A}_D)^H\cdot\mathbf{R}^{-1}\cdot\mathbf{A}_D. \tag{13}$$

The $\mathbf{B}$ matrix in (13) is invertible provided that the directions of the M_D desired signals are different (so that the $\mathbf{A}_D$ matrix has full rank) [9], in which case we obtain

$$\boldsymbol{\alpha}^{(s)} = \mathbf{B}^{-1}\cdot\boldsymbol{\zeta}. \tag{14}$$

Next, by substituting (14) and (11) in the Lagrangian (10), we obtain

$$\mathcal{L}\left(\mathbf{w}^{(s)};\boldsymbol{\alpha}^{(s)},\boldsymbol{\beta},\boldsymbol{\zeta}\right) = \boldsymbol{\zeta}^H\cdot\mathbf{B}^{-1}\cdot\boldsymbol{\zeta} - \sum_{m=1}^{M_D}\beta_m\left(|\zeta_m|^2-1\right). \tag{15}$$

As shown in the Appendix, the iterative scheme

$$\zeta_m^{(i+1)} = -\frac{\displaystyle\sum_{n=1,n\neq m}^{M_D}\left[\mathbf{B}^{-1}\right]_{mn}\zeta_n^{(i)}}{\left|\displaystyle\sum_{n=1,n\neq m}^{M_D}\left[\mathbf{B}^{-1}\right]_{mn}\zeta_n^{(i)}\right|} \tag{16}$$

converges to a minimum of the reduced Lagrangian in (15). The corresponding optimal weight vector $\mathbf{w}^{(opt)}$ is obtained substituting in (11) the converged values of (14) and (16). Note that, although there is no guarantee that the *global* minimum is reached, our numerical simulations (see Sect. 3) show that, as compared with global optimizers (such as, e.g., genetic algorithms [19]), the above iterative scheme provides a better tradeoff between MSE reduction and computational burden.

2.2. ANN Implementation

In order to approximate the complicated relationship between the input data and the optimal weight vector $\mathbf{w}^{(opt)}$ computed via the above MSE-minimization process, as in [16, 17], we choose a *radial basis function* (RBF) ANN implementation [20] in view of its effectiveness and versatility, as well as the ready availability of off-the-shelf software libraries their for creation, training, and simulation. Our architecture consists of an input layer, a hidden layer of Gaussian RBFs, and an output layer of summation nodes, and is designed using the following steps. First, for a given configuration of desired signals, we create a series of "examples" by: *i)* choosing (via uniform deterministic sampling) the angular directions of the interfering signals, *ii)* evaluating the ANN input data, and *iii)* computing the optimal weight $\mathbf{w}^{(opt)}$ via the proposed scheme. Subsequently, in order to have the ANN "learn" the underlying input-output mapping, we employ an appropriate RBF-ANN training procedure, based on the algorithm proposed in [21] and implemented in the `newrb` routine of the MATLAB Neural Network Toolbox [22], using the above examples as training data set. Following [16, 17], we choose as input of the ANN an N^2-dimensional real vector containing the (real and imaginary parts of the) elements of the upper triangular half of the correlation matrix $\mathbf{R}$ (in view of its symmetry), and as output a $(2N-1)$-dimensional real vector containing the (real and imaginary) components of the optimal weight vector $\mathbf{w}^{(opt)}$ (having assumed $w_1^{(opt)}$ purely real and positive in view of the degree of freedom in the choice of the phase reference). Additional theoretical and computational details regarding the RBF-ANN architecture and training can be found in [16, 17, 21].

2.3. Computational Burden

It is interesting to compare the computational burden of the proposed scheme with that of the standard one [16, 17]. In this connection, note that the computationally most expensive operation, performed in both

schemes, is the ANN training. The main computational difference in the two schemes lies in the creation of the training data sets, which, for the proposed scheme requires the additional minimization of the Lagrangian functional in (15) via the iterative procedure in (16). Accordingly, the proposed scheme requires an additional $\sim O(KM_D^2)$ burden, where K is the (M_D-dependent) number of iterations (16) required to achieve convergence. Recalling that, for $M \lesssim N$, the computational burden of the standard scheme [16, 17] is $\sim O(N^3)$, we can conclude that the additional burden is generally moderate, and becomes negligible for $M_D \ll N$.

3. REPRESENTATIVE RESULTS

In order to assess the effectiveness of the proposed scheme, we carried out an extensive parametric analysis and comparison with the standard scheme [16, 17].

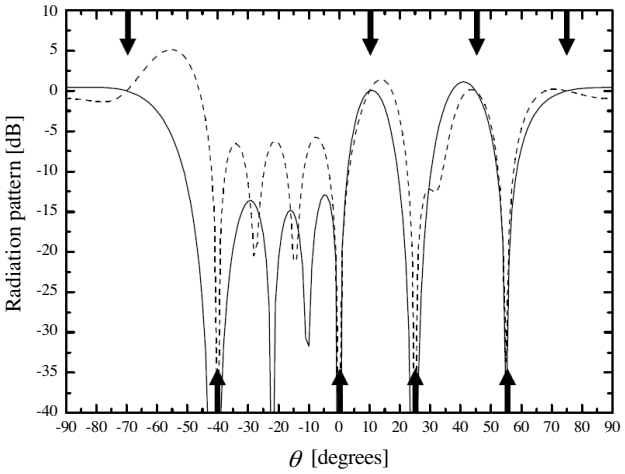

Figure 1. Examples of optimized radiation patterns obtained via the proposed (continuous curve) and standard (dashed curve) schemes, for a configuration featuring $N = 10$ array elements, $M_D = 4$ desired signals (with directions $\theta_1 = -70°$, $\theta_2 = 10°$, $\theta_3 = 45°$, $\theta_4 = 75°$, highlighted as thick arrows on the top axis), $M_I = 4$ interfering signals (with directions $\theta_5 = -40°$, $\theta_6 = 0, \theta_7 = 25°$, $\theta_8 = 55°$, highlighted as thick arrows on the bottom axis), SNR = 10 dB, and SIR = −10 dB.

First, we studied the performance at the input of the ANN. As an example, Fig. 1 shows the comparison between two typical

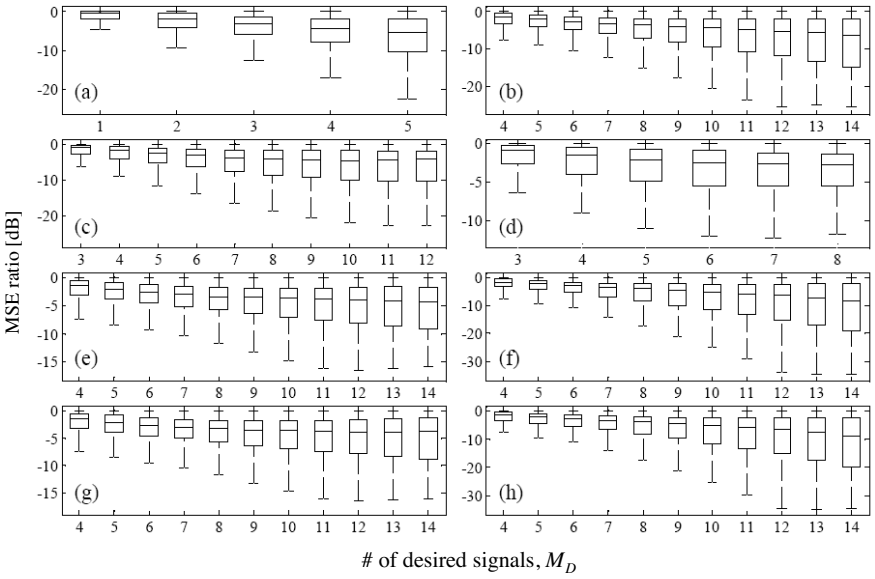

Figure 2. Boxplots of the statistics of the MSE ratio (proposed/standard) at the ANN input, as a function of the number of desired signals M_D, for various representative array and signal configurations. The statistics are obtained from sets of 10^5 examples characterized by random (uniform) arrival directions for the desired and interfering signals. (a): $N = 8$, $M_I = 2$, SNR $= 10$ dB, SIR $= -10$ dB; (b): $N = 16$, $M_I = 2$, SNR $= 10$ dB, SIR $= -10$ dB; (c): $N = 16$, $M_I = 4$, SNR $= 10$ dB, SIR $= -10$ dB; (d): $N = 16$, $M_I = 8$, SNR $= 10$ dB, SIR $= -10$ dB; (e): $N = 16$, $M_I = 4$, SNR $= 10$ dB, SIR $= -10$ dB; $N = 16$, $M_I = 2$, SNR $= 0$ dB, SIR $= -10$ dB; (f): $N = 16$, $M_I = 2$, SNR $= 20$ dB, SIR $= -10$ dB; (g): $N = 16$, $M_I = 2$, SNR $= 10$ dB, SIR $= 0$ dB; (h): $N = 16$, $M_I = 2$, SNR $= 10$ dB, SIR $= -20$ dB.

optimized radiation patterns obtained via the proposed and standard schemes, for a configuration featuring $N = 10$ array elements, $M_D = 4$ desired signals, $M_I = 4$ interfering signals, 10 dB signal-to-noise ratio (SNR $= \sigma^{-2}$), and -10 dB signal-to-interference ratio (SIR $= \Lambda^{-2}$). One observes, in both cases, the expected unit-gains and dip notches in the desired- and interfering-signal directions, respectively. While, at a *qualitative* glance, the proposed scheme appears more effective in lowering the gain in the angular regions away from the desired-signal directions, more *quantitative* and *statistically meaningful* assessments are clearly needed. In this framework, we generated, for representative

array and signal configurations, sets of 10^5 examples characterized by random (uniform) arrival directions for the desired and interfering signals, and looked at the ratio of the optimal MSEs in (5) obtained with the two schemes. The plots in Fig. 2, generated via the MATLAB `boxplot` function [22], compactly illustrate the salient features of the arising statistics. Basically, the ranges of the data are represented by the whiskers, and each box delimits the *interquartile range* (i.e., bottom= 25th percentile, and top = 75th percentile), with the horizontal line inside indicating the *median* (i.e., 50th percentile) value. Specifically, Figs. 2(a) and 2(b) show the MSE ratios pertaining to different number of array elements ($N = 8$ and $N = 16$, respectively) and desired signals M_D, for $M_I = 2$ interfering signals, and fixed values of the SNR and SIR. Different numbers of interfering signals are considered in Figs. 2(c) and 2(d) ($M_I = 4$ and $M_I = 8$, respectively), for a fixed number ($N = 16$) of array elements. Finally, different SNR and SIR values (spanning two decades) are considered in Figs. 2(e), 2(f) and 2(g), 2(h), respectively.

A number of remarks are in order. At a first *qualitative* glance, one observes that all the data ranges pertaining to the MSE ratios (proposed/standard) entirely fall within the negative dB scale, indicating that the proposed scheme *always* outperforms the standard one. This could be intuitively expected, as the optimal solution of the standard scheme also belongs to the search space of the proposed scheme ($\zeta_m = 1,\ m = 1, \ldots, M_D$), but was not to be taken for granted, since the convergence to the global minimum was not guaranteed for the proposed iterative optimization scheme in (16). In this connection, we also verified on a representative set of examples, that the use of a *global* optimizer (the `ga` routine in the MATLAB Genetic Algorithms Toolbox [22]) produced only slight (~ 0.1 dB, on average) improvements in the MSE reduction, at the expense of significant increases (nearly three orders of magnitude) in the computing times.

For more *quantitative* assessments, the interquartile and median parameters provide an immediate reading and interpretation of the statistical features. For instance, looking at Fig. 2(h), one readily observes that for the case of $M_D = 14$ desired signals the MSE improvement is $\gtrsim 10$ dB in 50% of the cases, and $\gtrsim 20$ dB in 25% of the cases.

The main general trends emerged from the parametric analysis can be summarized as follows:

- The proposed scheme becomes more effective with decreasing the difference $N - M_D$ between the number of elements and desired signals. This could be intuitively understood, recalling that for a small number of desired signals the degrees of freedom available

in the standard scheme could already suffice to achieve good MSE reduction.

- Increased effectiveness is also observed with increasing the SNR, and with decreasing the SIR.
- On the other hand, decreased effectiveness is observed for increasing number of interfering signals. This could be attributable to a correspondingly increased nonlinearity (i.e., number of local minima) of the arising optimization problem.

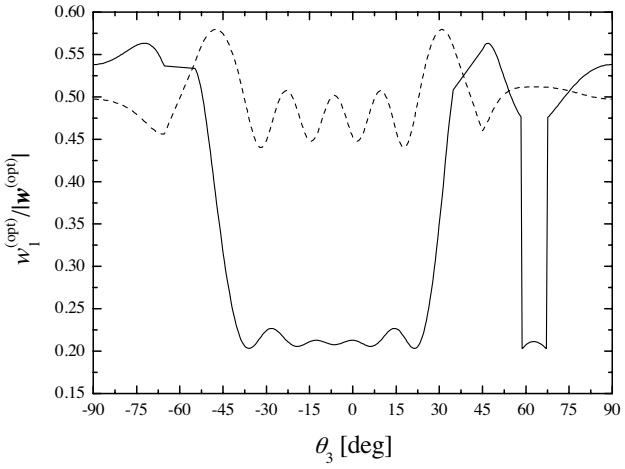

Figure 3. Normalized optimal weight coefficient $w_1^{(opt)}$ obtained via the proposed (continuous curve) and standard (dashed curve) schemes, for a configuration featuring $N = 8$, $M_D = 2$, $M_I = 1$, SNR = 10 dB, and SIR = −10 dB, as a function of the interfering-signal angular direction θ_3.

As a second step, we looked at the ANN implementation. In this connection, we carried out a preliminary study of the input-output mapping, in order to get insightful guidelines for the parameter choice. With reference to a simple configuration involving $N = 8$ array elements, $M_D = 2$ desired signals, and $M_I = 1$ interfering signal, Fig. 3 shows the behavior of the (real, positive) $w_1^{(opt)}$ optimal weight coefficient, as a function of the interfering-signal angular direction θ_3, obtained with the proposed and standard schemes. The behavior observed in the proposed scheme is considerably *more irregular* than the standard one, with the presence of several sharp jumps (see, e.g., around $\theta_3 = 60°$). Such markedly different behaviors, consistently observed in our preliminary study, imply that the proposed scheme

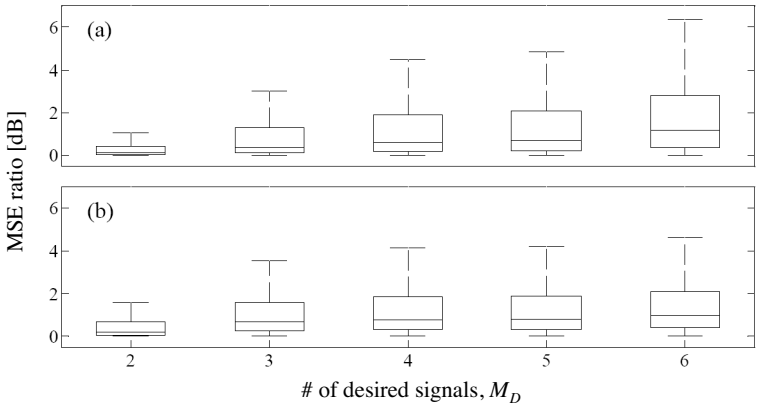

Figure 4. Input-output MSE ratio statistics pertaining to a RBF-ANN architecture (with 200 RBFs, and a training data set of 3000 examples) as a function of the number of desired signals, for a configuration featuring $N = 8$, $M_I = 2$, $\mathrm{SNR} = 10\,\mathrm{dB}$, $\mathrm{SIR} = -10\,\mathrm{dB}$. The statistics are obtained considering 30 different ANN realizations obtained varying (deterministically, via uniform sampling) the interfering-signal angular directions. (a): Proposed scheme; (b): Standard scheme.

requires a comparatively *more complex* ANN implementation in order to well approximate the input-output mapping. Although there exist alternative ANN architectures particularly suited for approximating discontinuous functions (see, e.g., [23, 24]), we found that standard RBF-ANNs can still yield acceptable results with a suitable increase in the number of RBFs. For a representative example involving $N = 8$ array elements and $M_I = 2$ interfering signals, Fig. 4 illustrates, for both the proposed and standard schemes, the input-output MSE ratio statistics pertaining to a RBF-ANN architecture (with 200 RBFs, and a training data set of 3000 examples) as a function of the number of desired signals. The statistics are obtained considering 30 different ANN realizations obtained varying (deterministically, via uniform sampling) the interfering-signal angular directions. One observes comparable levels of ANN-induced MSE deterioration for both cases, thereby concluding that the performance improvement attainable via the proposed scheme is generally preserved by the ANN implementation.

4. CONCLUSIONS

In this paper, we have presented and evaluated an adaptive beamforming scheme based on *magnitude-only* constraints and implementable via RBF-ANNs. Specifically, we have assessed, via an extensive parametric study, the potential improvements (in terms of MSE reduction) by comparison with a standard MSE-based approach, and addressed the underlying computational implications. Overall, the proposed scheme appears as an attractive alternative to the standard one, especially in the presence of a number of desired signals comparable with the number of array elements, with median improvements as large as $\sim 10\,\mathrm{dB}$ in the MSE reduction, at the expense of a moderate increase in the computational burden. Current and future investigations are aimed at the exploration of alternative ANN architectures particularly suited for approximating discontinuous mappings [23, 24].

APPENDIX A. ITERATIVE MINIMIZATION ALGORITHM

We can show that updating $\boldsymbol{\zeta}$ according to the iterative rule in (16) yields a non-increasing sequence of values of the reduced Lagrangian in (15). By using the equality $|\zeta_m| = 1$, $m = 1, \ldots, M_D$, the variation of $\mathcal{L}$ in (15), after updating the m-th state only, is given by

$$\Delta\mathcal{L}_m^{(i+1)} = 2\mathrm{Re}\left\{ \left[\zeta_m^{(i+1)} - \zeta_m^{(i)}\right]^* \sum_{n=1, n\neq m}^{M_D} \left[\mathbf{B}^{-1}\right]_{mn} \zeta_n^{(i)} \right\}, \qquad \text{(A1)}$$

with * denoting complex conjugation. By using (16), we obtain

$$\Delta\mathcal{L}_m^{(i+1)} = -2 \left| \sum_{n=1, n\neq m}^{M_D} \left[\mathbf{B}^{-1}\right]_{mn} \zeta_n^{(i)} \right| \left(1 + \cos\gamma_m^{(i)}\right), \qquad \text{(A2)}$$

where $\gamma_m^{(i)} = \arg\left[\zeta_m^{(i)} / \left(\sum_{n=1, n\neq m}^{M_D} [\mathbf{B}^{-1}]_{mn} \zeta_n^{(i)}\right)\right]$. Note that the right hand side of (A2) is non-positive and, as a result, the sequence $\mathcal{L}$ is *non-increasing*.

REFERENCES

1. Chryssomallis, M., "Smart antennas," *IEEE Antennas Propagat. Mag.*, Vol. 42, 129–136, 2000.

2. Bach-Andersen, J., H. Boche, A. Bourdoux, J. Fonollosa, T. Kaiser, and W. Utschick (eds.), *Smart Antennas: State of Art*, Hindawi, New York, NY, 2004.
3. Rabideau, D. J., "Clutter and jammer multipath cancellation in airborne adaptive radar," *IEEE Trans. Aerospace Electron. Syst.*, Vol. 36, 565–583, 2000.
4. Ray, J. K., M. E. Cannon, and P. Fenton, "Adaptive GPS code and carrier multipath mitigation using a multiantenna system," *IEEE Trans. Aerospace Electron. Syst.*, Vol. 37, 183–195, 2001.
5. Mouhamadou, M., P. Vaudon, and M. Rammal, "Smart antenna array patterns synthesis: Null steering and multi-user beamforming by phase control," *Progress In Electromagnetics Research*, PIER 60, 95–106, 2006.
6. Fakoukakis, F. E., S. G. Diamantis, A. P. Orfanides, and G. A. Kyriacou, "Development of an adaptive and a switched beam smart antenna system for wireless communications," *Journal of Electromagnetic Waves and Applications*, Vol. 20, 399–408, 2006.
7. Mukhopadhyay, M., B. K. Sarkar, and A. Chakraborty, "Augmentation of anti-jam GPS system using smart antenna with a simple DOA estimation algorithm," *Progress In Electromagnetics Research*, PIER 67, 231–249, 2007.
8. Mahmoud, K. R., M. El-Adawy, S. M. M. Ibrahem, R. Bansal, and S. H. Zainud-Deen, "A comparison between circular and hexagonal array geometries for smart antenna systems using particle swarm optimization algorithm," *Progress In Electromagnetics Research*, PIER 72, 75–90, 2007.
9. Bresler, Y., V. U. Reddy, and T. Kailath, "Optimum beamforming for coherent signal and interferences," *IEEE Trans. Acoust. Speech Signal Process.*, Vol. 36, 833–843, 1988.
10. Schmidt, R. O., "Multiple emitter location and signal parameter estimation," *IEEE Trans. Antennas Propagat.*, Vol. 34, 276–280, 1986.
11. Roy, R. and T. Kailath, "ESPRIT — Estimation of signal parameters via rotational invariance techniques," *IEEE Trans. Acoust. Speech Signal Process.*, Vol. 37, 984–995, 1989.
12. Haykin, S., *Neural Networks*, Mac-Millan, New York, NY, 1994.
13. Rayas-Sánchez, J. E., "EM-based optimization of microwave circuits using artificial neural networks: The state-of-the-art," *IEEE Trans. Microwave Theory Tech.*, Vol. 52, 420–435, 2004.
14. Ayestaran, R. G., F. Las-Heras, and J. A. Martinez, "Non

uniform-antenna array synthesis using neural networks," *Journal of Electromagnetic Waves and Applications*, Vol. 21, 1001–1011, 2007.

15. Mohamed, M. D. A., E. A. Soliman, and M. A. El-Gamal, "Optimization and characterization of electromagnetically coupled patch antennas using RBF neural networks," *Journal of Electromagnetic Waves and Applications*, Vol. 20, 1101–1114, 2006.
16. El Zooghby, A. H., C. G. Christodoulou, and M. Georgiopoulos, "Neural network-based adaptive beamforming for one-and two-dimensional antenna arrays," *IEEE Trans. Antennas Propagat.*, Vol. 46, 1891–1893, 1998.
17. El Zooghby, A. H., C. G. Christodoulou, and M. Georgiopoulos, "A neural-network-based linearly constrained minimum variance beamformer," *Microwave Opt. Technol. Lett.*, Vol. 21, 451–455, 1999.
18. Fletcher, R., *Practical Methods of Optimization*, Wiley, New York, NY, 1990.
19. Haupt, R. L. and D. H. Werner, *Genetic Algorithms in Electromagnetics*, Wiley-IEEE Press, Hoboke, NJ, 2007.
20. Park, J. and I. W. Sandberg, "Universal approximation using radial basis function networks," *Neural Comput.*, Vol. 3, 246–257, 1991.
21. Chen, S., C. F. N. Cowan, and P. M. Grant, "Orthogonal least squares learning algorithm for radial basis function networks," *IEEE Trans. Neural Networks*, Vol. 2, 302–309, 1991.
22. Higham, D. J. and N. J. Higham, *MATLAB Guide, SIAM*, Philadelphia, PA, 2005.
23. Zhang, M., S. Xu, and J. Fulcher, "Neuron-adaptive higher order neural-network models for automated financial data modeling," *IEEE Trans. Neural Networks*, Vol. 13, 188–204, 2002.
24. Rastko, R. and F. L. Lewis, "Neural-network approximation of piecewise continuous functions: Application to friction compensation," *IEEE Trans. Neural Networks*, Vol. 13, 745–751, 2002.